Mol Cell Biochem (2017) 436:167–178
DOI 10.1007/s11010-017-3088-8

Activation of adrenergic receptor in H9c2 cardiac myoblasts co-stimulates Nox2 and the derived ROS mediate the downstream responses

Nikhat Saleem[1] · Shyamal K. Goswami[1]

Received: 26 December 2016 / Accepted: 1 June 2017 / Published online: 7 June 2017

Abstract In recent years, NADPH oxidases (Noxes) have emerged as an important player in cardiovascular pathophysiology. Despite the growing evidences on the role of specific Nox isoforms, mechanisms of their activation, targets of reactive oxygen species (ROS) generated, and their downstream effects are poorly understood as yet. In this study, we treated H9c2 cardiac myoblasts with norepinephrine (NE, 2 μM), inducing ROS generation that was inhibited by Nox2-specific peptide inhibitor gp91ds-tat. Organelle-specific hydrogen peroxide-sensitive probe HyPer showed that the site of ROS generation is primarily in the cytosol, to some extent in the endoplasmic reticulum (ER) but not the mitochondria. Modulation of mRNAs of marker genes of cardiac hypertrophy i.e. induction in ANP and β-MHC, and reduction in α-MHC by NE treatment was prevented by specific inhibition of Nox2 by gp91ds-tat. Induction of ANP and β-MHC at the protein level were also attenuated by the inhibition of Nox2. Induction of c-Jun and FosB, the two members of the transcription factor family AP-1, were also blocked by the inhibition of Nox2 by gp91ds-tat. Induction of promoter-reporter constructs harboring multiple AP-1 elements and the upstream of FosB and ANP genes by NE were also blocked by the inhibition of Nox2 by gp91ds-tat and a dominant negative mutant of p22phox, a constituent of Nox2 that prevents its activation. This study for the first time establishes the significant role of Nox2 in mediating the NE-induced pathological adrenergic signaling in cardiac myoblasts.

Keywords Redox signaling · Reactive oxygen species · NADPH oxidase · Cardiac hypertrophy · Norepinephrine · gp91ds-tat

Introduction

Oxidative stress has long been attributed to cardiovascular diseases like endothelial dysfunction, cardiac hypertrophy, cardiomyocyte apoptosis, ischemia–reperfusion injury, and heart failure [1–3]. Paradoxically, alleviating those conditions by antioxidants has largely been unsuccessful [4]. Recent years have seen paradigm shifts wherein apart from their deleterious effects, reactive oxygen species (ROS) have emerged as the mediator of intracellular signals [5]. Such regulatory roles of ROS are fast evolving [6, 7]. Superoxide ($O_2^{\cdot-}$), a prevalent ROS, is generated from a number of redox enzymes and mitochondrial electron transport complexes in distinct cellular locations. It is also converted into hydrogen peroxide (H_2O_2), a potent signaling molecule [7]. Their effects on the cellular constituents depend on the duration of generation, steady-state concentrations, subcellular locations, and surrounding antioxidants [8, 9]. $O_2^{\cdot-}$ and H_2O_2 may oxidize, nitrosylate, or glutathionylate the cysteine thiols in adjoining proteins, affecting their conformation, stability, and functions [6, 10].

The response of the cardiovascular system to the pathological stimuli leading to the development of hypertrophy and heart failure is complex and involves all known modes of regulations including phosphorylation–dephosphorylation, intracellular trafficking, protein and mRNA

Electronic supplementary material The online version of this article (doi:10.1007/s11010-017-3088-8) contains supplementary material, which is available to authorized users.

✉ Shyamal K. Goswami
skgoswami@mail.jnu.ac.in; shyamal.goswami@gmail.com

[1] School of Life Sciences, Jawaharlal Nehru University, New Delhi 110067, India

turnover, and oxidative modifications of the cellular proteome [11]. While the other modes of regulation are better understood, those by the oxidative and nitrosative modifications of various proteins are least investigated till date [6, 11].

Norepinephrine (NE) is released from the sympathetic nervous system and targets α- and β-adrenergic receptors, regulating cardiac performance [12, 13]. Cardiac myocytes in culture when treated with a lower dose of NE (≤10 μM NE) elicit hypertrophic response, while at a higher dose (≥50 μM NE) induces apoptosis. These two responses are the hallmark of heart failure [14, 15]. We have demonstrated earlier that although ROS are the common denominators of both the responses, its mechanism of actions is far more nuanced and complex than simple threshold-dependent effects as perceived earlier [16, 17].

NADPH oxidases (Nox1-5) are enzymes solely dedicated for the production of $O_2^{\cdot-}$ and H_2O_2 in various tissues in a context-specific manner [18]. Except Nox4 which is constitutive, all other Noxes are activated by various mechanisms [19]. Apart from their activation by intracellular mechanisms like calcium flux and by protein–protein interactions, they are also co-activated by the engagement of various growth factors, peptide hormones, and cytokines to their cognate receptors, though the mechanisms are not fully understood [20–22]. Three of its isoforms viz., Nox1/2/4 are expressed in heart and ROS generated from them have been attributed to interstitial fibrosis, contractile dysfunction, ischemia–reperfusion injury, and cardiac remodeling [6, 11, 23, 24].

Nox2, the prototype member of the family, is primarily localized in the plasma membrane and it is involved in redox signaling from cell exterior to interior [25]. In heart, several pathophysiological stimuli, i.e., hypoxia, membrane depolarization (endothelial cells), induction of platelet activating factor (PAF), arachidonic acid, tumor necrosis factor-α (TNF-α), and interleukin-1β (IL-1β), activate Nox2 [23].

Despite evidences that generation of ROS is an integral part of adrenergic signaling, their source, nature, and mode of actions are largely unknown [16, 17, 26]. In the present study, we demonstrate that in H9c2 cardiac myoblasts, stimulation of adrenergic receptor by NE co-stimulates Nox2 generating $O_2^{\cdot-}$ and H_2O_2. ROS generated from Nox2 is an integral part of the adrenergic signaling as the inhibition of Nox2 prevents the activation of transcription factors mediating hypertrophic response and the induction of a number of marker genes considered as the hallmarks of hypertrophy.

Materials and methods

Reagents

All chemicals were purchased from Sigma-Aldrich, USA unless otherwise specified. Peptide inhibitor gp91ds-tat (*RKKRRQRRRCSTRIRRQL-NH2)* was obtained from AnaSpec, Inc. pHyPer-Cyto and pHyPer-Mito constructs were obtained from Evrogen (Moscow, Russia). p22-phox-Wt and p22-phox-DN constructs were kind gift from Dr. Jaharul Haque, Cleveland Clinic, USA [27]. Rabbit monoclonal antibodies against Fos-B, c-Jun, p–c-Jun, and GAPDH were purchased from Cell Signaling Technologies, USA. Rabbit polyclonal antibody against β-MHC was purchased from Biorbyt, UK. Mouse monoclonal antibody against ANP and Horseradish peroxidase-conjugated anti-mouse and anti-rabbit IgG antibodies were obtained from Santa Cruz Biotechnology, USA. Alexa fluor-555 goat anti-rabbit and Alexa fluor-488 goat anti-mouse secondary antibodies were procured from Thermo Fisher Scientific, US. All the oligonucleotides used for cloning and transcript level measurement were synthesized from Sigma-Aldrich (Supplemental Table 1).

Cell culture

H9c2 cardiac myoblasts were procured from Sigma-Aldrich, USA (originally from ECACC, UK) and were cultured as monolayer in Dulbecco's modified Eagle medium (DMEM) supplemented with 10% fetal bovine serum (FBS), 90 U/ml Penicillin, 90 μg/ml streptomycin and 5 μg/ml amphotericin B in humidified, 5% CO_2 containing incubator at 37 °C.

ROS/$O_2^{\cdot-}$ measurement

H9c2 cells were grown in 35-mm dish to 70% confluence and kept in serum-free media for 12–14 h followed by treatment with 2 μM NE for 10 min. Wherever necessary, cells were pretreated with gp91ds-tat peptide (5 μM), 30 min prior to NE treatment. Thirty minutes prior to imaging, cells were treated with the fluoroprobes Dichlorodihydro-fluorescein diacetate (DCFH-DA, 5 μM) or Dihydroethidium (DHE, 10 μM), kept in dark at 37 °C, and washed in PBS (phosphate buffer saline), and the images were captured in Nikon Eclipse Ti-E fluorescence microscope using excitation/emission at 504/529 and 535/610 nm, respectively. For quantification, the mean intensity of fluorescence was measured by NIS-Elements software (Nikon).

Construction of pHyPer-ER

For targeting HyPer to endoplasmic reticulum (ER), the HyPer-ER was reconstituted from HyPer-Cyto essentially as described by Malinouski et al. [28]. Briefly, an 87-nucleotide-long oligonucleotide harboring the ER signal peptide sequence of 29 amino acids was generated from the total RNA isolated from the pituitary gland of rat by using appropriate primers (supplemental Table 1). The PCR product was then cloned in frame at the N-terminal of pHyPer-Cyto. Also, in the C-terminal, a synthetic 12-nucleotide-long sequence harboring the ER retention signal (KDEL) was inserted. The strategy details are given in Supplemental Fig. 1s.

Measurement of cell compartment-specific H_2O_2 generation

H9c2 cells were grown in 35-mm glass bottom dish to 70% confluence followed by transient transfection using Escort IV transfection reagent according to the manufacturer's instructions. After 24 h of transfection, cells were kept in serum-free media for 12–14 h followed by treatment with 2 μM NE in phenol red free DMEM. Fluorescence of live cells was captured while in a live cell chamber with 5% CO_2 at 37 °C by Andor spinning disc confocal microscope (Olympus) with excitation using 488 nm laser line. The intensity of fluorescence was quantified by NIS-Elements AR-ver 4.000 software.

Gene expression analysis

H9c2 cells were grown to 70% confluence and kept in serum-free media for 12–14 h followed by 2 μM NE treatment. Wherever necessary, cells were also treated with gp91ds-tat peptide (5 μM) 30 min prior to NE treatment. After 24 h, total RNA was isolated using TRI reagent according to the manufacturer's instructions. One microgram of RNA was reverse transcribed using Applied Biosystems reverse transcription kit as per the manufacturer's protocol. Gene-specific primers were used to analyze the transcript level using SYBR green master mix (Applied Biosystems) in an Applied Biosystems 7500 real-time PCR system. Modulation of transcript levels was quantified using Ct values and normalization was done with the transcript level of the house keeping gene GAPDH.

Immunofluorescence analysis

H9c2 cells were grown on poly-L-lysine-coated coverslips in 12-well culture plate. Cells were treated with 2 μM NE and 5 μM gp91ds-tat peptide (30 min prior to NE treatment) wherever marked for indicated time point. After treatment time, cells were fixed with chilled methanol for 20 min followed by PBS washes and blocked with PBS containing 1% BSA, 1% bovine serum, and 0.1% Triton-X-100 for 60 min. Then, after PBS washes, the coverslips were incubated overnight at 4 °C with 1:100 rabbit-anti-β-MHC or mouse-anti-ANP or rabbit-anti-FosB antibodies diluted in blocking solution. Next day, after washing three times with PBS, cells were incubated with 1:500 Alexa fluor-555 goat anti-rabbit secondary antibody (red fluorescence) or Alexa fluor-488 goat anti-mouse secondary antibody (green fluorescence) for 60 min. After three washes in PBS, the coverslips were sealed with glass slides in 80% glycerol (in PBS) containing cell nuclei stain Hoechst (1:1000). The images were captured in Nikon Eclipse Ti-E fluorescence microscope at 60X magnification.

Immunoblot analysis

H9c2 cells were grown to 70% confluence and kept in serum-free media for 12–14 h followed by 2 μM NE treatment. Wherever necessary, cells were also treated with gp91ds-tat peptide (5 μM) 30 min prior to NE treatment. After indicated time points, cells were harvested in cold PBS followed by centrifuge at 3000 rpm for 15 min. The pellet obtained was lysed in RIPA buffer (50 mM Tris; pH 7.4, 150 mM NaCl, 1% Triton X-100, 1% sodium deoxycholate, 0.1% SDS, 1 mM EDTA) with phosphatase inhibitor cocktail, 1 mM phenylmethylsulfonyl fluoride (PMSF), and protease inhibitor cocktail followed by sonication. The homogenates were centrifuged and supernatant was assessed for protein concentration by the Bradford method using BSA as standard. Proteins were separated (50 μg per well) on 10 or 12% SDS-polyacrylamide gel and transferred onto PVDF membrane (Millipore, USA). Membranes were blocked with 3% BSA in 0.1% TBST for 2 h at room temperature followed by incubation with specific primary antibodies (diluted in 3% BSA in 0.1% TBST) at 4 °C overnight. Then the membrane was incubated with anti-rabbit or anti-mouse IgG secondary antibody conjugated to peroxidase (HRP) at 1:10,000 dilution in 0.1% TBST for 1 h at room temperature. Membranes were exposed to enhanced chemiluminescence reagent and visualized on X-ray film (Kodak, USA). Quantification of band intensities was performed with the Image-J software system. The signal intensity of each protein band was normalized with the corresponding GAPDH signal and fold change over control was calculated.

Analysis of promoter-reporter activity

H9c2 cells were grown to 70% confluence followed by transient transfection with reporter plasmids with or without

the co-transfection with p22-phox constructs using Escort IV transfection reagent as directed by the manufacturer. Cells were kept in serum-free medium for 12–14 h and treated with 2 μM NE and 5 μM gp91ds-tat peptide (30 min prior to NE treatment) wherever marked. The cells were harvested after 4 h of NE treatment in 1× lysis buffer (Promega), lysates were then analyzed for luciferase activity using the Luciferase Reagent Assay Kit (Promega) in accordance with the manufacturer's instructions in a GLOMAX Multi JR detection system (Promega). Normalization of transfection efficiency was done by the estimation of total protein used for the luciferase assay [29, 30].

Statistical analysis

Statistical analyses were performed using GraphPad Prism, PC version 5 (GraphPad software). Data are expressed as mean ± SEM. Each experiment was performed at least in triplicate. Experimental groups were compared with the use of one-way ANOVA if there was one independent variable (Tukey's test) or two-way ANOVA if there were two independent variables. Values of $P < 0.05$ were considered statistically significant.

Results

NE-treated cardiac myoblast generates ROS from Nox2

We have demonstrated earlier that cardiac myoblasts upon stimulation with NE generates a complex repertoire of ROS that contribute towards the downstream responses viz., hypertrophy and apoptosis [16, 17, 30]. Since such generation of ROS is an immediate (<1 min) response and includes both $O_2^{\cdot-}$ and H_2O_2, involvement of Nox2 is anticipated. To test this possibility, H9c2 cardiac myoblasts were kept in serum-free medium overnight and stimulated with NE (2 μM) for 10 min. Generation of ROS was monitored by the general ROS-sensitive fluoroprobe Dichloro-dihydro-fluorescein diacetate (DCFH-DA) and $O_2^{\cdot-}$-specific fluoroprobe Dihydroethidium (DHE). To test the involvement of Nox2, its specific peptide inhibitor gp91ds-tat (5 μM) was added. As shown in Fig. 1a, NE-induced ROS (DCFH-DA) generation was completely blocked by the specific inhibition of Nox2. In agreement with our previous report, part of the ROS was $O_2^{\cdot-}$ (DHE sensitive) that was also completely blocked by

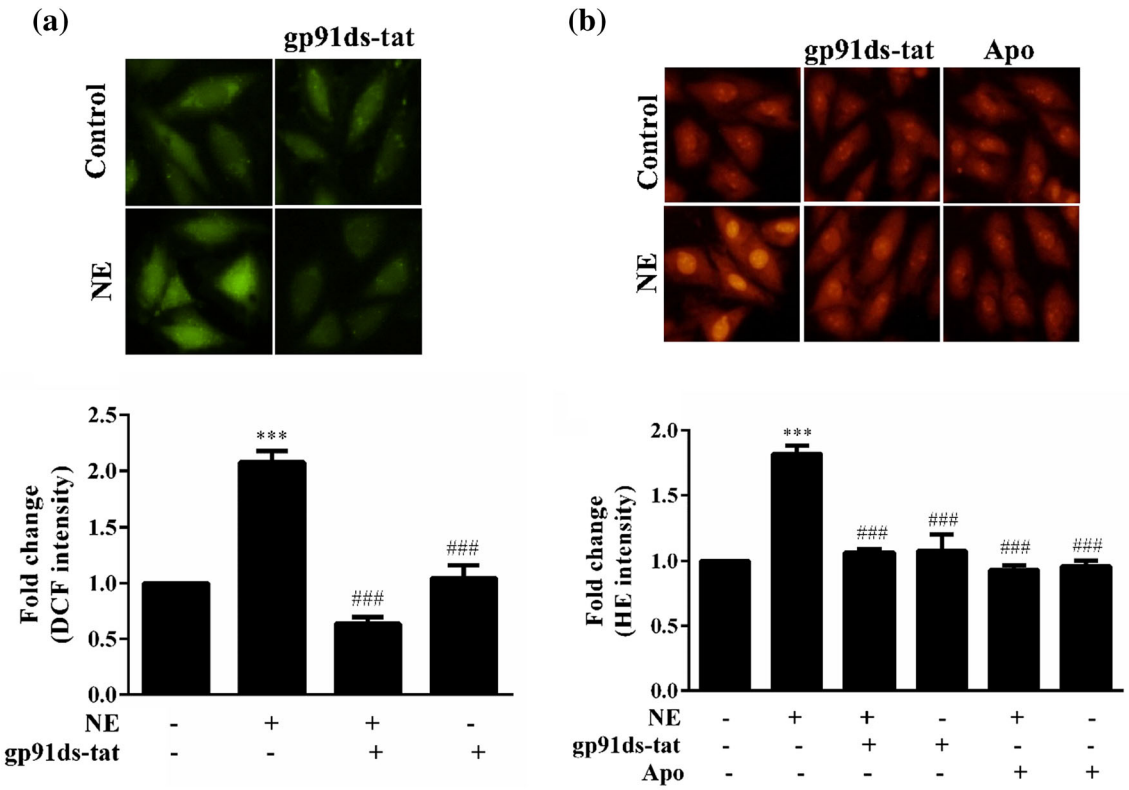

Fig. 1 Nox2 is the source of ROS in NE-treated cardiac myoblasts Upper panel: H9c2 cells were serum starved overnight followed by treatment with 2 μM NE for 10 min. 5 μM gp91ds-tat or 10 μM Apo was added 30 min before NE treatment wherever marked. Cells were labeled with **a** redox-sensitive fluoroprobe DCFH-DA (5 μM) or **b** superoxide-sensitive fluoroprobe DHE (10 μM), 30 min prior to imaging. *Lower Panel* quantification of the fluorescence intensity normalized to control. $^{***}P \leq 0.001$ versus control; $^{\#\#\#}P \leq 0.001$ versus NE

the specific inhibition of Nox2 by gp91ds-tat as well as the general inhibition of all Noxes by apocynin (Fig. 1b). These results strongly corroborated with our hypothesis that stimulation of adrenergic receptor by NE co-activates Nox2 and generates $O_2^{\cdot-}$ and other associated ROS.

NE induces ROS generation primarily in the cytosol

We have demonstrated earlier that treatment of H9c2 cardiac myoblasts with 2 μM of NE leads to the sustained but oscillating generation of ROS [16, 17, 30]. Since redox signaling is specified by the cellular microdomain where it is generated, we also tested the subcellular location of the ROS generated by NE. Cells were transfected with the H_2O_2-sensitive cpYFP (circularly permuted-yellow fluorescent protein)-based ratiometric fluorescent probe HyPer plasmids [31] that monitors the H_2O_2 generation in the cytoplasm, mitochondria, and endoplasmic reticulum (ER). After 24 h of transfection, cells were kept overnight in serum-free media followed by treatment with 2 μM NE and live cell imaging was done for 1 h at Ex_{max} 488 nm. As shown in Fig. 2a, snapshots of a single living cell showed treatment with NE resulted in a sharp and rapid increase in H_2O_2 generation in the cytosol, that sustained till 1 h, the last time point tested (further analysis was not possible as the cells started crumbling, presumably due to the repeated exposure to the light). Although there was a gradual decrease (∼20%) in fluorescence with time, it was still well above the baseline (untreated cells). Noticeably, no increase in fluorescence was seen in the mitochondria in NE-treated cells as monitored by the HyPer-Mito (Fig. 2b). Rather, the signal was below the baseline (untreated control) after 30 min, though the reason is not clear. The efficacy of the assay was evident from the increase in fluorescence in cells treated with 20 μM H_2O_2. Unlike the mitochondria, some increase in fluorescence was seen in ER upon NE treatment (Fig. 2c), though the response was not as intense as in cytosol. The higher baseline intensity of HyPer-ER reflects the oxidizing environment of ER. Together, these data suggest that cytosol is the primary and the ER is the secondary location of H_2O_2 generation in NE-treated cells. Due to the lack of organelle-specific probes, similar assay for superoxide generation in those organelles could not be done.

Induction of fetal gene expression by NE is prevented by the inhibition of Nox2

Re-induction of fetal gene expression program is a characteristic feature of cardiac hypertrophy and it is faithfully reproduced by treating cultured myocytes ex vivo with adrenergic agonists [32, 33]. To analyze the role of Nox2-induced ROS in the induction of fetal gene program if any, we estimated the mRNA levels of three established markers viz., ANP (atrial natriuretic peptide), α-MHC (α-myosin heavy chain), and β-MHC (β-myosin heavy chain). As expected, upon treatment with 2μ NE, the transcript levels of ANP and β-MHC increased by ∼1.7 and 2.0 fold, respectively, and that of α-MHC decreased by ∼0.4 fold. Pretreatment of cells with gp91ds-tat (5 μM) prevented the modulation of transcript levels by NE (Fig. 3a). We further confirmed such modulation of hypertrophic markers at the protein levels by immunocytochemistry. As shown in Fig. 3b, treatment with NE (2 μM) increased the levels of both ANP and β-MHC that were attenuated by the inhibition of Nox2 by gp91ds-tat (5 μM). These results not only strengthened our previous observation that ROS induced by NE treatment play a direct role in regulation of gene expression in hypertrophied heart [16, 17, 30], it also established that Nox2 is the primary source of this regulatory ROS (Figs. 1, 2).

Nox2-induced ROS modulate the activities of transcription factors mediating hypertrophic responses

Heterodimeric transcription factor AP-1 has long been identified as the key mediator of hypertrophic signals elicited by several agonists [34]. Also, depending on the pathophysiological stimuli, the role of AP-1 can be divergent [35]. We have demonstrated earlier that in NE-treated cardiac myoblasts, the redox and kinase signals integrate at various transcription factors viz, AP-1, SP-1, and CREB, which then mediate their effects through the cognate *cis*-regulatory elements in the responsive gene promoters, specifying the transcriptional output [16, 30]. To reiterate that observation in the context of ROS generated from Nox2, the expression levels of two members of the AP-1 family that is c-Jun and FosB were assayed by Western analysis. As shown in Fig. 4a (left panel), upon treatment with NE, c-Jun level was induced by 1.25 and 1.38 fold at 2 and 4 h of NE treatment, respectively, and that were attenuated by gp91ds-tat treatment. Although, gp91ds-tat itself also showed some induction of c-Jun, it was less than that able to suppress the c-Jun level below baseline at 4 h. Similar observations were also made for FosB (FBJ murine osteosarcoma viral oncogene homolog B), a member of the AP-1 family and the dimerization partner of c-Jun. As shown in Fig. 4a (left panel), level of FosB was increased by 1.45 fold in NE-treated cells at 2 h but diminished thereafter at 4 h. This kinetic is in agreement with our earlier study with the FosB transcript [30]. As expected, the induction of FosB was also abrogated by treatment with gp91ds-tat. In view with the low intensity of the signal with the FosB antibody in the Western blot (possibly, a reflection of the low abundance), we also confirmed its

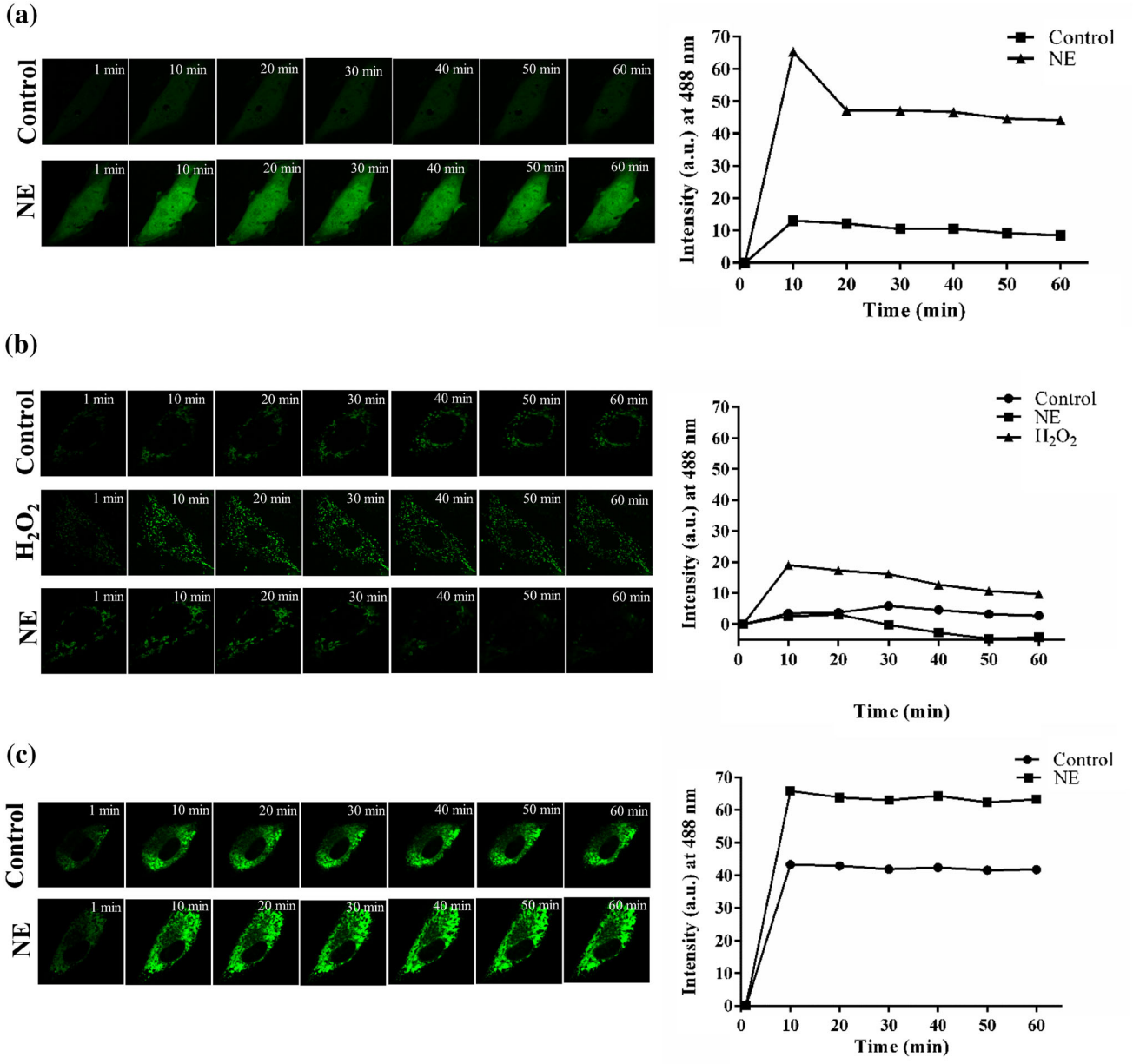

Fig. 2 NE induces generation of hydrogen peroxide primarily in the cytosol Left panel: H9c2 cells were transfected with **a** pHyPer-Cyto, **b** pHyPer-Mito, and **c** pHyPer-ER. After 24 h of transfection, cells were kept overnight in serum-free media followed by treatment with 2 μM NE or 20 μM H_2O_2 treatment as marked. Live single cell imaging was done at 60X for 1 h at Ex_{max} 488 nm and most representative image is shown. *Right panel* quantification of the fluorescence intensity normalized to intensity at 1 min

modulation by immunocytochemistry as shown on the right panel. Immunocytochemistry not only reiterated the pattern of modulation seen in the Western blot, it also showed the nuclear localization of FosB. We also examined the level of phospho-c-Jun in NE-treated cells and its modulation by gp91ds-tat. As shown in Fig. 4a (left panel), treatment with NE rather decreased the level of phospho-c-Jun (thus effectively decreasing the phospho-c-Jun/c-Jun ratio) while treatment with gp91ds-tat partially restored that reduction. Although, phosphorylation of c-jun is known for its activation (in addition to the increase in its expression level), its cellular function is highly context specific with multiple layers of a regulatory networks wherein it integrates different signals [36]. It is thus difficult to assess the implication of increase in c-Jun expression with concurrent decrease in its state of phosphorylation upon NE treatment. Nevertheless, these data unequivocally reiterate that Nox2 plays a role in modulating the AP-1 activity by NE. Subsequent to analyzing the expression of c-Jun and FosB, we also assayed a number of promoter-reporter (luciferase)

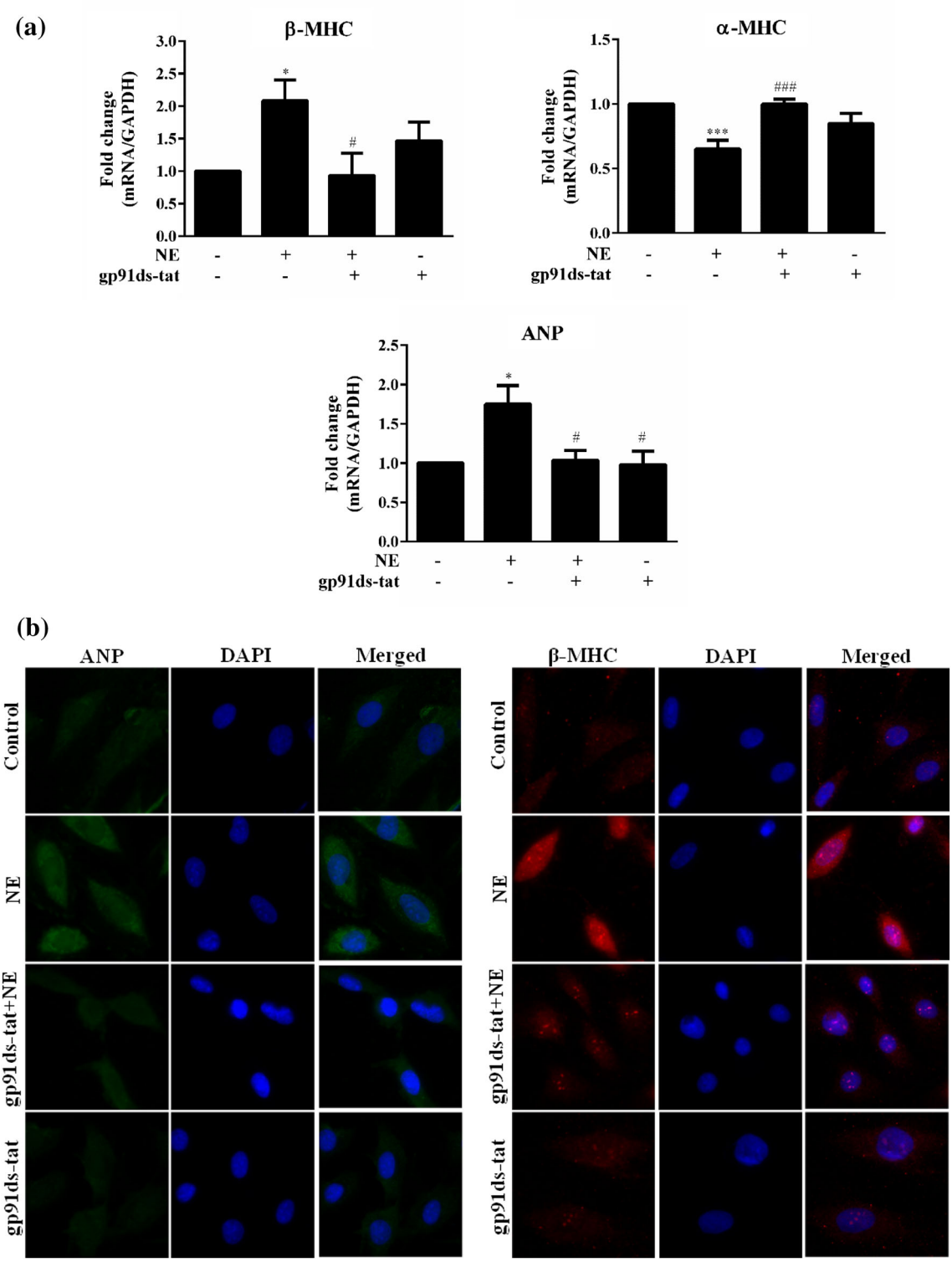

Fig. 3 Induction of fetal gene expression by NE is prevented by the inhibition of Nox2 H9c2 cells were serum starved overnight followed by treatment with 2 μM NE for 24 h. 5 μM gp91ds-tat was added 30 min before NE treatment wherever marked. **a** Total RNA was assayed for ANP, β-MHC, and α-MHC transcripts using gene-specific primers by Real-time PCR. Normalization of input RNA was done by using GAPDH level as an internal control. Fold differences of mRNA levels over control were calculated. **b** Immunostaining was done using antibody specific for ANP (*left panel*) and β-MHC (*right panel*). $^{*}P \leq 0.05$ versus control; $^{***}P \leq 0.001$ versus control; $^{\#}P \leq 0.05$ versus NE; $^{\#\#\#}P \leq 0.001$ versus NE

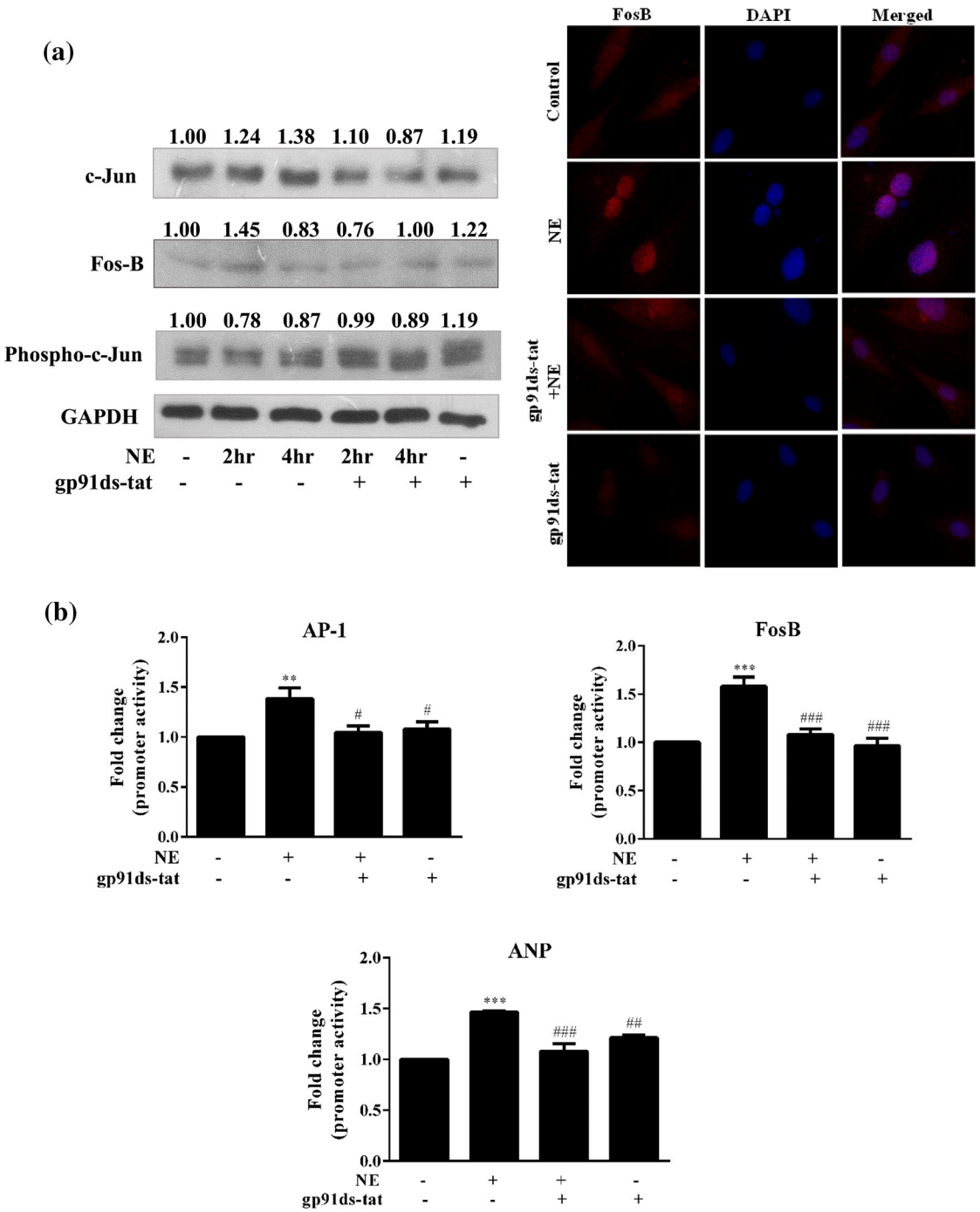

Fig. 4 Nox2-induced ROS modulate the activities of transcription factors mediating the hypertrophic response **a** H9c2 cells were serum starved overnight followed by treatment with 2 μM NE for 2 or 4 h as indicated. 5 μM gp91ds-tat was added 30 min before NE treatment wherever marked. *Left panel* Total protein was isolated and equal amount (50 μg) of lysates were assayed by Western blot analysis using antibody specific for FosB, Phospho-c-Jun, and c-Jun. GAPDH level was the loading control. The intensity of bands was evaluated as a ratio relative to that of GAPDH and values are written above the respective bands. Most representative image out of three independent experiment is shown. *Right panel* Immunostaining was done using antibody specific for FosB. H9c2 cells were **b** transfected with AP-1, FosB, and ANP promoter-reporter constructs either alone **c** or co-transfected with p22-phox-Wt or p22-phox-DN constructs. After 24 h of transfection, cells were kept overnight in serum-free media followed by treatment with 2 μM NE for 4 h. 5 μM gp91ds-tat was added 30 min before NE treatment wherever marked. Cell lysates were assayed for reporter luciferase activity. Normalization of luminescence was done against total protein concentration. Fold differences of promoter activity over control were calculated. $^{**}P \leq 0.01$ versus control; $^{***}P \leq 0.001$ versus control; $^{\#}P \leq 0.05$ versus NE; $^{\#\#}P \leq 0.01$ versus NE; $^{\#\#\#}P \leq 0.001$ versus NE $^{\$\$\$\$}P \leq 0.0001$ versus p22-phox-Wt untreated; $^{\$\$\$}P \leq 0.001$ vs p22-phox-Wt untreated; $^{\$}P \leq 0.05$ versus p22-phox-DN untreated

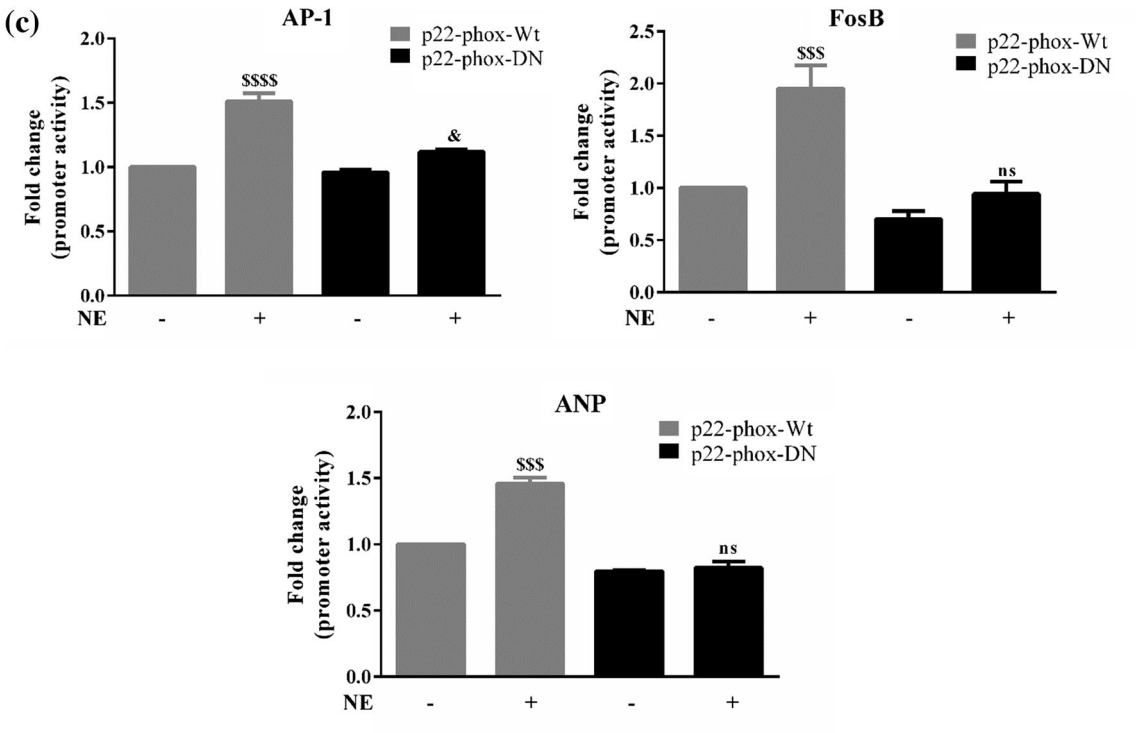

Fig. 4 continued

constructs regulated by AP-1 in cardiac myocytes treated with adrenergic agonists. We tested one synthetic promoter harboring three consecutive AP-1 binding sites, and two endogenous promoters viz that of ANP and FosB genes. The endogenous promoter of ANP gene has been extensively studied for analyzing the signal transduction pathways mediating hypertrophic response [37] and it harbors an AP-1 site along with other cis-elements [38]. Although the FosB promoter has not been studied in details, we have demonstrated that it is selectively activated by the hypertrophic dose of NE and have used it as a paradigm of understanding how redox and kinase signals integrate at the gene level regulating its expression [16, 30]. When we tested the effects of NE on these promoters, there was increase by ~1.45 fold for AP-1, ~1.6 fold for FosB, and ~1.5 fold for ANP. Pretreatment of cells with the Nox2 inhibitor gp91ds-tat (5 μM) prevented the induction of all three (Fig. 4b).

To further confirm the role of Nox2 in regulating the expression of these promoters in NE-treated cells, we co-transfected the wildtype (Wt) and the dominant negative (DN) variants of p22-phox subunit of Nox. Although the activation of both Nox2/4 isoforms requires p22-phox, its DN variant (P156Q) prevents ROS generation from Nox2 only [19, 27]. We argued that if the upregulation of these promoters are Nox2 dependent, it would be compromised by the over-expression by the DN mutant of p22-phox. As shown in Fig. 4c, expression of p22-phox-DN subunit of Nox compromised the stimulatory effect of NE seen in control, that is promoters transfected with the p22-phox-Wt, confirming the involvement of Nox2 in mediating NE response. Taken together, these data reiterate the involvement of Nox2 in modulating the gene network involved in hypertrophic signaling by NE.

Discussion

While the specificity of kinase signaling is directed by protein–protein interactions, that of redox signaling depends on multiple factors like the localization of the reactive species in subcellular microdomain, the pKa of neighboring cysteine thiols, surrounding antioxidants, and the presence of free transition metals [39, 40]. Redox signaling in mammalian cell is thus highly nuanced, calibrated, and difficult to dissect.

Among the three Noxes present in heart, function of Nox4 is better investigated. Its activation by multiple stimuli including ischemia–reperfusion, pressure overload, and energy starvation vis-à-vis its location in the mitochondria, ER, and the nucleus exemplifies the complexity of redox signaling in cardiac pathobiology [41]. On the contrary, the role of Nox2, the prototype Nox, in cardiac function is lesser understood, even though its activation by pressure volume overload and early preconditioning has been reported [41, 42]. The functioning of the cardiovascular system is

modulated by a plethora of growth factors, cytokines, and hormones, but adrenergic signaling plays a nodal role in these processes. Therefore, our observation that in cardiac myoblasts, the activation of adrenergic receptors co-stimulates Nox2 is novel and significant as it gives a new dimension to the adrenergic signaling.

Although ROS have been implicated in all major pathological conditions in heart, its sources and potential targets are largely unknown [1–4, 23, 24, 43]. We have documented earlier that once the ROS generation is stimulated by NE, it sustains independently, presumably by some yet unknown downstream mechanisms [16, 17]. As the present study shows that the ROS generated by NE treatment is completely attenuated by the selective inhibition of Nox2, it is thus the only source of ROS at the onset. Although the primary product of Nox2 is $O_2^{\cdot-}$, it can be immediately converted into H_2O_2 by intra- and extracellular SOD (superoxide dismutase), and the chemistry of signaling by these two ROS is quite different. We therefore tested the nature of ROS generated by Nox2 and the presence of both $O_2^{\cdot-}$ and H_2O_2 were detected in NE-treated cells. These results are in full agreement with our earlier observation that upon NE treatment, H9c2 cardiac myoblasts generate a complex mixture of $O_2^{\cdot-}$, H_2O_2, and other secondary ROS, although their sources were unknown in earlier study [17]. In this study, we also for the first time demonstrated that H_2O_2 generated by Nox2 is primarily localized in the cytosol, to some extent in the ER but completely absent in the mitochondria. Among various organelles, mitochondria have generally been viewed as the principal source of ROS in heart, especially under pathological conditions [41, 42], although cytosolic, endoplasmic reticular, and nuclear ROS have also been attributed to the cardiac pathobiology [23, 44–46]. Further study on the targets of cytosolic H_2O_2 in mediating the downstream signals will be of immense interest.

Although the cross-talk between the redox and kinase signaling has long been envisaged, the mechanistic insights are highly inadequate [7, 47]. We had demonstrated earlier how kinase and redox signals generated in NE-treated cardiac myoblasts are integrated at multiple *cis* regulatory elements in the target genes [30]. In reiteration, we now demonstrate that three prototype genes for hypertrophic response viz., ANP, β-, and α-MHC; modulated by NE remained to their baseline levels by the selective inhibition of Nox2. This observation further exemplifies the seamless integration of the ROS and kinase signaling we had demonstrated earlier [30]. Such integration is further confirmed by the prevention of the induction of the one promoter exclusively regulated by the transcription factors AP-1, and two others, i.e., of ANP and FosB, considered as the prototype of adrenergic signaling; upon selective inhibition of Nox2. Although the specific inhibition of Nox2 by the peptide inhibitor gp-91-ds-tat has been shown by numerous studies [48], considering our emphasis on the pivotal role of Nox2 in adrenergic signaling, we also validated our claim by using a dominant negative mutant of p22phox which hampers the generation of ROS from Nox2 isoform only. This mutant also completely blocked the induction of FosB, ANP, and AP-1 promoters induced by NE. The rational for using these promoters for the validation of Nox2 signaling is that these are at the end points of the kinase and ROS signals generated at the cell surface by the ligand, i.e., NE.

Taken together, our study firmly establishes the close interaction between the conventional kinase signaling from the adrenergic receptors and the emergent ROS signaling from Nox2 as the key mediator of adrenergic responses in the cardiac myoblasts.

Acknowledgements This work was supported by The Department of Biotechnology, Government of India, under Grant (BT/PR4268/BRB/10/1016/2011), awarded to SKG. NS is a recipient of a JRF/SRF from the Indian Council of Medical Research, Government of India.

Compiance with ethical standards

Ethical approval This article does not contain any studies performed with animals.

References

1. Ho E, Karimi Galougahi K, Liu C-C et al (2013) Biological markers of oxidative stress: applications to cardiovascular research and practice. Redox Biol 1:483–491. doi:10.1016/j.redox.2013.07.006
2. Murray TVA, Ahmad A, Brewer AC (2014) Reactive oxygen at the heart of metabolism. Trends Cardiovasc Med 24:113–120. doi:10.1016/j.tcm.2013.09.003
3. Zhang Y, Tocchetti CG, Krieg T, Moens AL (2012) Oxidative and nitrosative stress in the maintenance of myocardial function. Free Radic Biol Med 53:1531–1540. doi:10.1016/j.freeradbiomed.2012.07.010
4. Sawyer DB (2011) Oxidative stress in heart failure: what are we missing? Am J Med Sci 342:120–124. doi:10.1097/MAJ.0b013e3182249fcd
5. Wadley AJ, Aldred S, Coles SJ (2016) An unexplored role for Peroxiredoxin in exercise-induced redox signalling? Redox Biol 8:51–58. doi:10.1016/j.redox.2015.10.003
6. Forman HJ, Ursini F, Maiorino M (2014) An overview of mechanisms of redox signaling. J Mol Cell Cardiol 73:2–9. doi:10.1016/j.yjmcc.2014.01.018
7. Latimer HR, Veal EA (2016) Peroxiredoxins in regulation of MAPK signalling pathways; sensors and barriers to signal transduction. Mol Cells 39:40–45. doi:10.14348/molcells.2016.2327
8. Lee J-G, Baek K, Soetandyo N, Ye Y (2013) Reversible inactivation of deubiquitinases by reactive oxygen species in vitro and in cells. Nat Commun 4:1568. doi:10.1038/ncomms2532

9. Stangherlin A, Reddy AB (2013) Regulation of circadian clocks by redox homeostasis. J Biol Chem 288:26505–26511. doi:10.1074/jbc.R113.457564
10. Groitl B, Jakob U (2014) Thiol-based redox switches. Biochim Biophys Acta 1844:1335–1343. doi:10.1016/j.bbapap.2014.03.007
11. Madamanchi NR, Runge MS (2013) Redox signaling in cardiovascular health and disease. Free Radic Biol Med 61:473–501. doi:10.1016/j.freeradbiomed.2013.04.001
12. Ciccarelli M, Santulli G, Pascale V et al (2013) Adrenergic receptors and metabolism: role in development of cardiovascular disease. Front Physiol 4:265. doi:10.3389/fphys.2013.00265
13. Ferrara N, Komici K, Corbi G et al (2014) β-adrenergic receptor responsiveness in aging heart and clinical implications. Front Physiol 4:396. doi:10.3389/fphys.2013.00396
14. Clerk A (2003) The radical balance between life and death. J Mol Cell Cardiol 35:599–602
15. Fu Y-C, Chi C-S, Yin S-C et al (2004) Norepinephrine induces apoptosis in neonatal rat cardiomyocytes through a reactive oxygen species-TNF alpha-caspase signaling pathway. Cardiovasc Res 62:558–567. doi:10.1016/j.cardiores.2004.01.039
16. Gupta MK, Neelakantan TV, Sanghamitra M et al (2006) An assessment of the role of reactive oxygen species and redox signaling in norepinephrine-induced apoptosis and hypertrophy of H9c2 cardiac myoblasts. Antioxid Redox Signal 8:1081–1093. doi:10.1089/ars.2006.8.1081
17. Thakur A, Alam MJ, Ajayakumar MR et al (2015) Norepinephrine-induced apoptotic and hypertrophic responses in H9c2 cardiac myoblasts are characterized by different repertoire of reactive oxygen species generation. Redox Biol 5:243–252. doi:10.1016/j.redox.2015.05.005
18. Sirokmány G, Donkó Á, Geiszt M (2016) Nox/Duox family of NADPH oxidases: lessons from knockout mouse models. Trends Pharmacol Sci 37:318–327. doi:10.1016/j.tips.2016.01.006
19. von Löhneysen K, Noack D, Wood MR et al (2010) Structural insights into Nox4 and Nox2: motifs involved in function and cellular localization. Mol Cell Biol 30:961–975. doi:10.1128/MCB.01393-09
20. Heppner DE, van der Vliet A (2016) Redox-dependent regulation of epidermal growth factor receptor signaling. Redox Biol 8:24–27. doi:10.1016/j.redox.2015.12.002
21. Spencer NY, Engelhardt JF (2014) The basic biology of redoxosomes in cytokine-mediated signal transduction and implications for disease-specific therapies. Biochemistry (Mosc) 53:1551–1564. doi:10.1021/bi401719r
22. Brandes RP, Weissmann N, Schröder K (2014) Nox family NADPH oxidases: molecular mechanisms of activation. Free Radic Biol Med 76:208–226. doi:10.1016/j.freeradbiomed.2014.07.046
23. Granger DN, Kvietys PR (2015) Reperfusion injury and reactive oxygen species: the evolution of a concept. Redox Biol 6:524–551. doi:10.1016/j.redox.2015.08.020
24. Lassègue B, San Martín A, Griendling KK (2012) Biochemistry, physiology, and pathophysiology of NADPH oxidases in the cardiovascular system. Circ Res 110:1364–1390. doi:10.1161/CIRCRESAHA.111.243972
25. Fisher AB (2009) Redox signaling across cell membranes. Antioxid Redox Signal 11:1349–1356. doi:10.1089/ars.2008.2378
26. Theccanat T, Philip JL, Razzaque AM et al (2016) Regulation of cellular oxidative stress and apoptosis by G protein-coupled receptor kinase-2; The role of NADPH oxidase 4. Cell Signal 28:190–203. doi:10.1016/j.cellsig.2015.11.013
27. Kawahara T, Ritsick D, Cheng G, Lambeth JD (2005) Point mutations in the proline-rich region of p22phox are dominant inhibitors of Nox1- and Nox2-dependent reactive oxygen generation. J Biol Chem 280:31859–31869. doi:10.1074/jbc.M501882200
28. Malinouski M, Zhou Y, Belousov VV et al (2011) Hydrogen peroxide probes directed to different cellular compartments. PLoS One 6:e14564. doi:10.1371/journal.pone.0014564
29. Burch PM, Yuan Z, Loonen A, Heintz NH (2004) An extracellular signal-regulated kinase 1- and 2-dependent program of chromatin trafficking of c-Fos and Fra-1 is required for cyclin D1 expression during cell cycle reentry. Mol Cell Biol 24:4696–4709. doi:10.1128/MCB.24.11.4696-4709.2004
30. Jindal E, Goswami SK (2011) In cardiac myoblasts, cellular redox regulates FosB and Fra-1 through multiple cis-regulatory modules. Free Radic Biol Med 51:1512–1521. doi:10.1016/j.freeradbiomed.2011.07.008
31. Belousov VV, Fradkov AF, Lukyanov KA et al (2006) Genetically encoded fluorescent indicator for intracellular hydrogen peroxide. Nat Methods 3:281–286. doi:10.1038/nmeth866
32. Banerjee P, Bandyopadhyay A (2014) Cytosolic dynamics of annexin A6 trigger feedback regulation of hypertrophy via atrial natriuretic peptide in cardiomyocytes. J Biol Chem 289:5371–5385. doi:10.1074/jbc.M113.514810
33. Yariswamy M, Yoshida T, Valente AJ et al (2016) Cardiac-restricted overexpression of TRAF3 interacting protein 2 (TRAF3IP2) results in spontaneous development of myocardial hypertrophy, fibrosis, and dysfunction. J Biol Chem 291:19425–19436. doi:10.1074/jbc.M116.724138
34. Yan L, Zhang JD, Wang B et al (2013) Quercetin inhibits left ventricular hypertrophy in spontaneously hypertensive rats and inhibits angiotensin II-induced H9C2 cells hypertrophy by enhancing PPAR-γ expression and suppressing AP-1 activity. PLoS One 8:e72548. doi:10.1371/journal.pone.0072548
35. Windak R, Müller J, Felley A et al (2013) The AP-1 transcription factor c-Jun prevents stress-imposed maladaptive remodeling of the heart. PLoS One 8:e73294. doi:10.1371/journal.pone.0073294
36. Meng Q, Xia Y (2011) c-Jun, at the crossroad of the signaling network. Protein Cell 2:889–898. doi:10.1007/s13238-011-1113-3
37. Wang J, Paradis P, Aries A et al (2005) Convergence of protein kinase C and JAK-STAT signaling on transcription factor GATA-4. Mol Cell Biol 25:9829–9844. doi:10.1128/MCB.25.22.9829-9844.2005
38. Knowlton KU, Baracchini E, Ross RS et al (1991) Co-regulation of the atrial natriuretic factor and cardiac myosin light chain-2 genes during alpha-adrenergic stimulation of neonatal rat ventricular cells. Identification of cis sequences within an embryonic and a constitutive contractile protein gene which mediate inducible expression. J Biol Chem 266:7759–7768
39. Dey S, Sidor A, O'Rourke B (2016) Compartment-specific control of reactive oxygen species scavenging by antioxidant pathway enzymes. J Biol Chem 291:11185–11197. doi:10.1074/jbc.M116.726968
40. Schaar CE, Dues DJ, Spielbauer KK et al (2015) Mitochondrial and cytoplasmic ROS have opposing effects on lifespan. PLoS Genet 11:e1004972. doi:10.1371/journal.pgen.1004972
41. Maejima Y, Kuroda J, Matsushima S et al (2011) Regulation of myocardial growth and death by NADPH oxidase. J Mol Cell Cardiol 50:408–416. doi:10.1016/j.yjmcc.2010.12.018
42. Bell RM, Cave AC, Johar S et al (2005) Pivotal role of NOX-2-containing NADPH oxidase in early ischemic preconditioning. FASEB J Off Publ Fed Am Soc Exp Biol 19:2037–2039. doi:10.1096/fj.04-2774fje
43. Montezano AC, Touyz RM (2014) Reactive oxygen species, vascular Noxs, and hypertension: focus on translational and clinical research. Antioxid Redox Signal 20:164–182. doi:10.1089/ars.2013.5302

44. Jang S, Lewis TS, Powers C et al (2016) Elucidating mitochondrial electron transport chain supercomplexes in the heart during ischemia-reperfusion. Antioxid Redox Signal. doi:10.1089/ars.2016.6635
45. Qin F, Siwik DA, Pimentel DR et al (2014) Cytosolic H2O2 mediates hypertrophy, apoptosis, and decreased SERCA activity in mice with chronic hemodynamic overload. Am J Physiol Heart Circ Physiol 306:H1453–H1463. doi:10.1152/ajpheart.00084.2014
46. Matsushima S, Kuroda J, Zhai P et al (2016) Tyrosine kinase FYN negatively regulates NOX4 in cardiac remodeling. J Clin Investig 126:3403–3416. doi:10.1172/JCI85624
47. Burgoyne JR, Rudyk O, Cho H et al (2015) Deficient angiogenesis in redox-dead Cys17Ser PKARIα knock-in mice. Nat Commun 6:7920. doi:10.1038/ncomms8920
48. Derochette S, Serteyn D, Mouithys-Mickalad A et al (2015) EquiNox2: a new method to measure NADPH oxidase activity and to study effect of inhibitors and their interactions with the enzyme. Talanta 144:1252–1259. doi:10.1016/j.talanta.2015.08.007